

DOKUZ EYLÜL UNIVERSITY
GRADUATE SCHOOL OF NATURAL AND APPLIED
SCIENCES

A STUDY ON THERMAL CONDUCTIVITY OF
POLYMER NANOCOMPOSITES

by
Melis ÇOLAK

October, 2011
İZMİR

A STUDY ON THERMAL CONDUCTIVITY OF POLYMER NANOCOMPOSITES

**A Thesis Submitted to the
Graduate School of Natural and Applied Science of Dokuz Eylül University In
Partial Fulfillment of the Requirements for the Degree of Master Science in
Mechanical Engineering, Energy Program**

**by
Melis ÇOLAK**

**October, 2011
İZMİR**

M.Sc THESIS EXAMINATION RESULT FORM

We have read the thesis entitled "A STUDY ON THERMAL CONDUCTIVITY OF POLYMER NANOCOMPOSITES" completed by MELİS ÇOLAK under supervision of PROF. DR. İSMAİL HAKKI TAVMAN and we certify that in our opinion it is fully adequate, in scope and in quality, as a thesis for the degree of Master of Science.



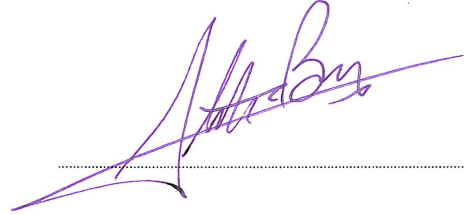
Prof. Dr. İsmail Hakkı TAVMAN

Supervisor



Assist. Prof. Dr. Alpaslan TURGUT

(Jury Member)



Assist. Prof. Dr. Tahsin BAŞARAN

(Jury Member)



Prof. Dr. Mustafa SABUNCU

Director

Graduate School of Natural and Applied Sciences

ACKNOWLEDGEMENTS

I would like to thank to my supervisor Prof. Dr. İsmail Hakkı Tavman for his invaluable advices, inestimable support and guidance.

I wish to express my gratefulness to Assist. Prof. Dr. Alpaslan Turgut for his incomparable helps, encouragement and invaluable support during the whole thesis.

I especially would like to thank to Prof. Dr. Olivier Fudym, Henrique Massard da Fonseca, PhD student, Denis Marty, technician and Ecole des Mines d'Albi's staff for their helps during the experiments.

I also would like to express my thanks to Dokuz Eylül University Mechanical Engineering department staff and students for their invaluable support.

Finally, i would like to thank to my family, my relatives, my friends and to my lover for their endless support, patience and giving meaning to my life..

Melis ÇOLAK

A STUDY ON THERMAL CONDUCTIVITY OF POLYMER NANOCOMPOSITES

ABSTRACT

In this work, graphite powder (400 nm) which has high thermal conductivity was mixed with HDPE in the Brabender Plasticorder mixer in certain conditions. Nanocomposites containing (2, 3, 4, 5, 6, 7, 10, 16 percent) volume fractions of graphite were fabricated. Thermal conductivity of high-density polyethylene (HDPE)-graphite nanocomposites is investigated experimentally and the results are compared with the theoretical models. A Hot-disk method is used to measure the thermal conductivity of nanocomposites consisting (2, 3, 4, 5, 6, 7, 10, 16 percent) volume fractions of high-density polyethylene (HDPE) matrix filled with graphite. Up to 6 percent volume of graphite, Russell model predict the thermal conductivity best.

Also the surface morphology of the polymer nanocomposites was searched by scanning electron microscopy (SEM) in different magnifications and it can be said that graphite particles dispersed almost homogenously in polymer matrix.

Keywords: Polymer nanocomposite, thermal conductivity, HDPE, graphite, hot-disk

POLİMER NANOKOMPOZİTLERİN ISIL İLETKENLİĞİNİN ÇALIŞILMASI

ÖZ

Bu çalışmada, yüksek ısı iletkenlik değerine sahip grafit tozu (400 nm) ile yüksek yoğunluklu polietilen (YYPE) Brabender Plasticorder cihazında belirli koşullar altında karıştırılmış ve yüzde (2, 3, 4, 5, 6, 7, 10, 16) hacimsel katkı oranlarında nanokompozitler üretilmiştir. YYPE-grafit nanokompozitin ısı iletkenliği deneysel olarak araştırılmış ve teorik modellerle karşılaştırılmıştır. Yüzde (2, 3, 4, 5, 6, 7, 10, 16) hacimsel katkı oranlarındaki yüksek yoğunluklu polietilen (YYPE)-grafit nanokompozitin ısı iletkenlikleri Hot-Disk metoduyla ölçülmüştür. Yüzde 6 grafit hacimsel katkı oranına kadar Russell ısı iletkenlik modeli deneysel verilerimizle uyuşmaktadır.

Ayrıca üretilen polimer nanokompozitlerin yüzey özellikleri elektron tarama mikroskopuyla farklı büyütme oranlarında belirlenmiş ve grafit parçacıklarının polimer matris içerisinde homojene yakın bir şekilde dağıldığı gözlemlenmiştir.

Anahtar sözcükler: Polimer Nanokompozit, Isı İletim Katsayısı, YYPE, Grafit, Hot-Disk

CONTENTS

| | Page |
|---|-------------|
| M.SC THESIS EXAMINATION RESULT FORM..... | ii |
| ACKNOWLEDGEMENTS | iii |
| ABSTRACT..... | vi |
| ÖZ | v |
| | |
| CHAPTER ONE - INTRODUCTION | 1 |
| | |
| 1.1 Introduction | 1 |
| 1.2 Polymer Nanocomposites..... | 5 |
| 1.2.1 Thermophysical Properties of Polymer Nanocomposites..... | 7 |
| | |
| CHAPTER TWO - THERMAL CONDUCTIVITY MODELS | 8 |
| | |
| CHAPTER THREE - THERMAL CONDUCTIVITY MEASURING METHODS | 12 |
| | |
| 3.1 Introduction | 12 |
| 3.2 Thermal Conductivity Measuring Methods | 13 |
| 3.2.1 Steady State Methods..... | 13 |
| 3.2.1.1 Guarded Hot Plate | 14 |
| 3.2.1.2 Concentric Cylinder | 14 |
| 3.2.1.3 Concentric Sphere | 15 |
| 3.2.2 Transient State Methods | 16 |
| 3.2.2.1 Fitch Method | 16 |

| | |
|--|-----------|
| 3.2.2.2 Probe Method | 16 |
| 3.2.2.3 3- ω Method | 17 |
| 3.2.2.4 Laser Flash method | 18 |
| 3.2.2.5 Hot-Disk Method | 21 |
| CHAPTER FOUR - MATERIALS AND METHODS | 26 |
| 4.1 Materials and Methods | 26 |
| 4.1.1 HDPE/Graphite | 26 |
| 4.1.2 Measurement Method and Apparatus | 29 |
| 4.1.3 Experimental Set-up | 31 |
| CHAPTER FIVE - RESULTS AND DISCUSSION..... | 37 |
| CHAPTER SIX - CONCLUSIONS AND FUTURE REMARK | 42 |
| REFERENCES..... | 43 |

CHAPTER ONE

INTRODUCTION

1.1 Introduction

In recent years, with increasing development in technology, many materials (polymers, metals, ceramics etc.)'s properties (electrical, mechanical, thermal etc.) need much more attention to be improved. Polymers (polyethylene (PE), polypropylene (PP), polyvinyl chloride (PVC), polyamide etc.) play a very important role in numerous fields of everyday life (electronics, textile, health, transportation etc.) due to their advantages over conventional materials (e.g. wood, clay, metals) such as lightness, resistance to corrosion, ease of processing and low cost production. Besides, polymers are easy to handle and have many degrees of freedom for controlling their properties, further improvement of their performance, including composite fabrication, still remains under intensive investigation. The altering and enhancement of the polymers properties can occur through doping with various nanofillers such as metals, semiconductors, organic and inorganic particles and fibers, as well as carbon structures and ceramics. Such additives are used in polymers for a variety of reasons, for example: improved processing, density control, optical effects, thermal conductivity, control of the thermal expansion, electrical properties that enable charge dissipation or electromagnetic interference shielding, magnetic properties, flame resistance, and improved mechanical properties, such as hardness, elasticity and tear resistance. (Pradhan, 2010, p.10)

In many studies polymer nanocomposites' thermal properties were investigated such as in the study of Kumlutas, Tavman & Coban (2003), high density polyethylene(HDPE)/aluminum(Al) composite's thermal measurements are obtained with hot-wire method. The thermal conductivity values are compared with several thermal conductivity models and with the numerical results. Numerical results, experimental values and all the models are close to each other at low particle content. For particle content greater than 10%, the effective thermal conductivity is exponentially formed. All the models fail to predict thermal conductivity in this

region. But, numerical results give satisfactory values in the whole range of aluminum particle content.

Tavman (1998) studied that experimental results of HDPE/tin (Sn) composites showed a region of low particle content, up to about 10% volume concentration, where the increase in thermal conductivity is rather slow. The filler particles are dispersed in the matrix material in this region, the thermal conductivity is best predicted by Maxwell's model and Nielsen's model with $A=1.5$, $\phi_m=0.637$. Whereas, at high filler concentrations, the filler particles tend to form agglomerates and conductive chains in the direction of heat flow resulting in a rapid increase in thermal conductivity. A model developed by Agari and Uno estimates the thermal conductivity in this region, using two experimentally determined constants.

Tekce, Kumlutas & Tavman (2007) studied with polyamide and copper(Cu) particles (fiber, spherical, prismatic). When the concentration value of 10 vol% is exceeded, a rapid increase in the thermal conductivity for the copper fiber filled polymer composite can be seen, which does not occur for the spherical or prismatic copper filled polymer composites. This rapid increase in the thermal conductivity can obviously be attributed to initiation of the interactions between the copper fibers, which is unlikely for the other types of fillers just after exceeding the 10 vol% filler concentration. In the Tlili, Boudenne, Cecen, Ibos, Krupa & Candau (2010)'s study, an increase of thermal conductivity (λ) with increasing filler content was observed for all samples investigated. This increase of λ is foreseeable because the filler has a significantly higher thermal conductivity than the polymeric matrix. It is also seen that EVA/UG composites have a higher thermal conductivity than the EVA/EG ones at the same concentration. For a given concentration, the filler size and the aspect ratio affect the heat propagation in the composite.

Krupa, Novák & Chodák (2004) investigated HDPE/graphite and LDPE/graphite composites. The thermal conductivity of composites nonlinearly increases with an increase in graphite content. The thermal conductivity of filled HDPE is higher than thermal conductivity of filled LDPE in the whole concentration range due to higher

degree of crystallinity of high density polyethylene. Generally, the most inorganic fillers have much higher thermal conductivity, than polymers and therefore their incorporation in the material leads to an increase in thermal conductivity of composites. Unfortunately, a prediction of thermal conductivity of filled polymers is very difficult and depends on geometry and orientation of filler particles in the matrix, concentration of the filler, ratio between thermal conductivity of the filler and thermal conductivity of the matrix. On the base of these factors, many different models have been already developed, but none of them has general validity, since the most of the model are derived for regular shape of particles, flakes or fibers as well as uniform distribution of their size.

Krupa & Chodak (2001) worked on thermal and electrical conductivity, thermal diffusivity of HDPE, polystyrene (PS) matrixs with different types of graphite(different distribution of particle size, different specific surface). Also mechanical properties were investigated. The thermal conductivity of HDPE is higher than thermal conductivity of PS. Semicrystalline matrices have higher both thermal conductivity and thermal diffusivity compared to amorphous matrices, since crystalline phase (regular structure) enables a better transport of heat than amorphous phase. The composites filled with graphite KS have higher thermal conductivity than composite filled with graphite EG at the same concentration. Since thermal conductivity of both types of graphite is the same, it's assumed that this fact is caused by higher aggregation of smaller graphite KS particles. The aggregates could improve a heat transport in the materials and improve thermal conductivity. Electrical conductivity measurements showed that different types of graphite have a different influence on the percolation concentration of composites. The percolation filler concentration was found to be lower in semicrystalline matrix (HDPE) compared to amorphous matrix (PS). In an PS matrix percolation concentration does not depend on characteristics of the filler particles (particle size) while in semicrystalline matrix (HDPE) different values have been found for two graphite particles differing in surface area. Similar behaviour was observed for thermal conductivity and thermal diffusivity. Mechanical properties are influenced by

reinforcing effect of the both fillers. The extent depends on the filler surface area, as indicated by increase in Young's modulus and decrease in elongation at break data.

In the Ye, Shentu & Weng (2005)'s study, the effect of the grade, the content, and the particle diameter on the thermal conductivity of HDPE filled with graphite were examined. The results show an increase of thermal conductivity of the HDPE/graphite composite with increase of graphite content. The thermal conductivity of the HDPE filled with the expanded graphite(EG) was larger than that of the HDPE filled with the colloid graphite system. At the same volume content (7%), the thermal conductivity of the former was twice that of the latter one. The particle diameter of the graphite also affected the thermal conductivity of HDPE composites. With increase of the particle diameter of the colloid graphite, the thermal conductivity of the HDPE/graphite increased. However, when the particle diameter of colloid graphite was larger than 15 μm , the increase of thermal conductivity of HDPE/graphite changed by inches. Some models proposed to predict thermal conductivity of a composite in a two-phase system could not be applied to HDPE filled graphite powder composites, such as Maxwell-Eucken, Cheng and Vachon, Zieblend, Lewis and Nielsen, Agari and Uno equations. But, according to the increase of thermal conductivity of HDPE composites filled with the colloid graphite, we find that Ziebland equation basically agrees with the experimental data for a wide range from 0% to 22% volume content of graphite. The advantages of thermal conductive polymer composites over metals are induced density, increased corrosion, oxidation, and chemical resistance; increased processability. However, polymers have disadvantages, for example, creep, thermal instability, and a limited number of processing techniques. The propagating rate of the thermal flow through a nonmetallic solid depends on the coupling intensity of the vibration movements of the atoms and groups of adjacent atoms. Intense couplings occur in the materials with covalent bonds, the thermal transmission showing a slight deficit in the case of highly ordered crystalline networks. In the case of graphite, the process of thermal energy transmission from one point to another, by means of atomic vibration, contributes to thermal conduction of HDPE filled with graphite. With the increase of volume content of graphite, many graphite particles touch each other to begin to

form graphite conductive chains, which may connect one electrode with the other. So the thermal conductivity of the HDPE/graphite composites increased. Thus, galleries of expanded graphite can be easily intercalated by suitable high-density polyethylene. Thermal conduction systems containing expanded graphite are “attached” systems in which expanded graphite particles interact with each other and affect the position of expanded graphite particles. Hence, thermal conductivities of HDPE filled with expanded graphite are prior to that of HDPE filled with colloid graphite.

Published values of thermal conductivities of the same filler materials in the same polymer matrices vary more or less for each study; this is mainly due to the mode of sample preparation as some samples are prepared by compression molding, some others by extrusion and injection molding. The size and shape of the filler, the volume fraction and also the interconnectivity of the filler particles in the matrix may be other factors which influence the thermal conductivities of the composites. (Kumlutaş & Tavman, 2006, Sanada, Tada & Shindo, 2009) Pradhan (2010) “The high thermal conductivity can be achieved by dispersing the nanoparticles in suitable methods. The high aspects ratio, high quality and well dispersed filler materials have much more enhancement in thermal conductivity.” (p.13)

In this study, polymer nanocomposite’s thermal conductivity fabricated from HDPE/graphite powder was measured with hot-disk method and the results are compared with the theoretical models. Our motivation is that although in many studies HDPE/graphite nanocomposites were examined, their thermal conductivity values weren’t taken with hot-disk method.

1.2 Polymer Nanocomposites

Polymer nanocomposites can be defined as polymers containing fillers with one dimension smaller than 100 nm. In contrast to traditional polymer composites with high loadings (60 vol.%) of micrometer-sized filler particles, polymer nanocomposites are being developed with very low loadings (less than 5 vol.%) of

well-dispersed nanofillers. While elastomeric composites with nanoscale spherical fillers have been in use for more than 100 years, in the last 15 years, new fillers have emerged, providing an opportunity for the development of high-performance multifunctional nanocomposites. For example, transparent conducting polymer/nanotube composites are under development as solar cell electrodes, nanoparticle filled amorphous polymers are being used as scratch-resistant, transparent coatings in cell phone and compact-disc technology. Nanoparticles are being considered for enhancing matrix properties of traditional composites to increase out-of-plane properties and add conductivity and sensing capabilities. The recent resurgence of interest in polymer nanocomposites has emerged for several reasons. First, nanoscale fillers often have properties that are different from the bulk properties of the same material. For example, as the size of silicon nanoparticles decreases, the band gap changes and the color of the particles changes. As another example, singlewall carbon nanotubes can exhibit stiffness, strength, and strain-to-failure that substantially exceeds that of traditional micrometer-diameter carbon fiber. These features of nanoparticles provide an opportunity for creating polymer composites with unique properties. Second, nanoscale fillers are small defects. Micrometer-scale fillers are similar in size to the critical crack size causing early failure while nanofillers are an order of magnitude smaller. This can prevent early failure, leading to nanocomposites with enhanced ductility and toughness. Similarly it has been shown that nanoparticles can increase the electrical breakdown strength and endurance and are small optical scattering defects. Third, due to the large surface area of the fillers, nanocomposites have a large volume of interfacial matrix material with properties different from the bulk polymer. One of the challenges in developing polymer nanocomposites for advanced technology applications is a limited ability to predict the properties. While the techniques exist to tailor the surface chemistry and structure of nanoparticle surfaces, the impact of the nanoscale filler surface on the morphology, dynamics, and properties of the surrounding polymer chains cannot be quantitatively predicted. Therefore, the properties of a significant volume fraction of the polymer, the interfacial polymer, are unknown making it difficult to predict bulk properties. (Schadler, Brinson & Sawyer, 2007)

1.2.1 Thermophysical Properties of Polymer Nanocomposites

Thermophysical properties can be simply defined as material properties that vary with temperature without altering the material's chemical identity. However, it has become customary to limit the scope of the term to properties having a bearing on the transfer and storage of heat. A more comprehensive definition is that thermophysical properties are all material properties affecting the transfer and storage of heat, that vary with the state variables temperature, pressure and composition (in mixtures), and of other relevant variables, without altering the material's chemical identity. These properties will include thermal conductivity and diffusivity, heat capacity, thermal expansion and thermal radiative properties, as well as viscosity and mass and thermal diffusion coefficients, speed of sound, surface and interfacial tension in fluids. (Thermophysical properties, 2011)

In the study of Aljaafari, Ibrahim & Brolossy (2010) they investigated the thermophysical behaviour of composites based on PVC filled with SWNT up to 3.65 vol% and they obtained properties such as thermal conductivity, thermal effusivity, thermal diffusivity using photoacoustic technique. They discovered that these properties were increased with the rising concentration of SWCNT.

Tlili et al.(2010) studied on EVA filled with nanostructuralized expanded graphite and standard, (nano)/micro-sized graphite. They measured thermal conductivity and thermal diffusivity for each composite at various filler concentrations. The thermophysical properties of these nanocomposites are higher than for the neat matrix. However, the filler size and the aspect ratio affect the heat propagation in the composite and the thermophysical behavior. Besides, it was shown that the structure of the graphite affects also the electrical behavior and the electrical percolation threshold, which in EVA/EG composites was found to be 6 vol% and 17 vol% in EVA/UG composites. In many reports with the increasing volume fraction of the filler, composites' thermal properties improved.

CHAPTER TWO

THERMAL CONDUCTIVITY MODELS

Many theoretical and empirical models have been proposed to predict the effective thermal conductivity of two-phase mixtures. For a two-component composite, the simplest alternatives would be with the materials arranged in either parallel or series with respect to heat flow, which gives the upper or lower bounds of effective thermal conductivity. (Kumlutas et al, 2003)

For the parallel conduction model:

$$k_c = \phi.k_f + (1 - \phi).k_m \quad (2.1)$$

c: composite; m: matrix; f: filler; ϕ : volume fraction of filler

For series conduction model:

$$\frac{1}{k_c} = \frac{\phi}{k_f} + \frac{1 - \phi}{k_m} \quad (2.2)$$

In the case of geometric mean model, the effective thermal conductivity of the composite is given by:

$$k_c = k_f^\phi . k_m^{(1-\phi)} \quad (2.3)$$

Lewis and Nielsen modified the Halpin-Tsai equation to include the effect of the shape of the particles and the orientation or type of packing for a two phase system:

$$k_c = k_m \frac{1 + A \cdot \beta \cdot \phi}{1 - \beta \cdot \phi \cdot \psi} \quad (2.4)$$

$$\beta = \frac{k_f/k_m - 1}{k_f/k_m + A} \quad \text{and} \quad \psi = 1 + \frac{1 - \phi_m}{\phi_m^2} \phi$$

Table 2.1 Value of A for various systems (Kumrlutas et al, 2003)

| Type of dispersed phase | Direction of heat flow | A |
|--|-------------------------|------------------|
| Cubes | Any | 2.0 |
| Spheres | Any | 1.5 |
| Aggregates of spheres | Any | $(2.5/\phi_n)-1$ |
| Randomly oriented rods <i>Aspect ratio = 2</i> | Any | 1.58 |
| Randomly oriented rods <i>Aspect ratio = 4</i> | Any | 2.08 |
| Randomly oriented rods <i>Aspect ratio = 6</i> | Any | 2.8 |
| Randomly oriented rods <i>Aspect ratio = 10</i> | Any | 4.93 |
| Randomly oriented rods <i>Aspect ratio = 15</i> | Any | 8.38 |
| Uniaxially oriented fibers | Parallel to fibers | 2L/D |
| Uniaxially oriented fibers | Perpendicular to fibers | 0.5 |

Table 2.2 Value of ϕ_n for various systems (Kumlutas et al, 2003)

| Shape of particle | Type of packing | ϕ_n |
|-------------------|--------------------------|----------|
| Spheres | Hexagonal close | 0.7405 |
| Spheres | Face centered cubic | 0.7405 |
| Spheres | Body centered cubic | 0.6 |
| Spheres | Simple cubic | 0.524 |
| Spheres | Random close | 0.637 |
| Rods or fibers | Uniaxial hexagonal close | 0.907 |
| Rods or fibers | Uniaxial simple cubic | 0.785 |
| Rods or fibers | Uniaxial random | 0.82 |
| Rods or fibers | Three dimensional random | 0.52 |

Tsao derived an equation relating the two phase solid mixture thermal conductivity of the individual components and two parameters which describe the spatial distribution of the two phases. By assuming a parabolic distribution of the discontinuous phase in the continuous phase (Figure 2.1), Cheng and Vachon obtained a solution to Tsao's model that did not require knowledge of additional parameters. The constants of this parabolic distribution were determined by analysis and presented as a function of the discontinuous phase volume fraction. Thus, the equivalent thermal conductivity of the two phase solid mixture was derived in terms of the distribution function and the thermal conductivity of the constituents:

$$\frac{1}{k_c} = \frac{1}{\sqrt{C \cdot (k_f - k_m)(k_m + B \cdot (k_f - k_m))}} \ln \frac{\sqrt{k_m + B(k_f - k_m)} + \frac{B}{2}\sqrt{C \cdot (k_f - k_m)}}{\sqrt{k_m + B \cdot (k_f - k_m)} - \frac{B}{2}\sqrt{C \cdot (k_f - k_m)}} + \frac{1-B}{k_m} \quad (2.5)$$

$$B = \sqrt{\frac{3 \cdot \phi}{2}} \quad , \quad C = -4 \cdot \sqrt{\frac{2}{3 \cdot \phi}}$$

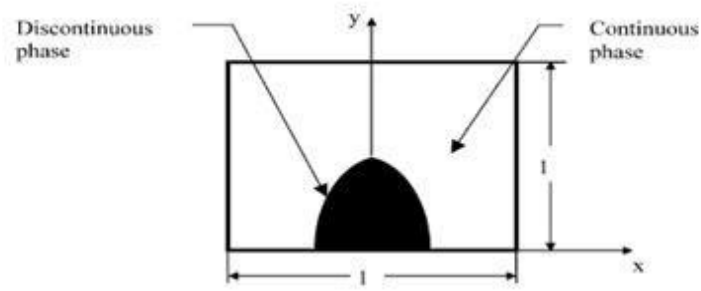


Figure 2.1 Parabolic distribution of the discontinuous phase for the Cheng and Vachon model.

Maxwell, using potential theory, obtained an exact solution for the conductivity of randomly distributed and non-interacting homogeneous spheres in a homogeneous medium. By solving Laplace's equation, he determined the effective conductivity of a random suspension of spheres within a continuous medium. The model developed by Maxwell assumes that the particles are sufficiently far apart that the potential around each sphere will not be influenced by the presence of other particles. (Kumlutas et al, 2003)

$$k_c = k_m \frac{k_f + 2.k_m + 2.\phi.(k_f - k_m)}{k_f + 2.k_m - \phi.(k_f - k_m)} \quad (2.6)$$

Assuming the pores are cubes of the same size and the isothermal lines are planes, Russell obtained the conductivity using a series parallel network:

$$k_c = k_m \left[\frac{\phi^{2/3} + \frac{k_m}{k_f} (1 - \phi^{2/3})}{\phi^{2/3} - \phi + \frac{k_m}{k_f} (1 + \phi - \phi^{2/3})} \right] \quad (2.7)$$

In this study the models that mentioned above are taken as comparative models for experimental results.

CHAPTER THREE

THERMAL CONDUCTIVITY MEASURING METHODS

3.1 Introduction

Heat conduction is molecular interchange of kinetic energy or electron drift. In molecular interchange, the molecules of the material are set into motion as they heated. In electron drift, heat conduction is primarily associated with the mobility of free electrons. In both cases, heat is transferred. Thermal conductivity is a measure of a material's ability to transmit heat. Unsteady state temperature distribution within a body subject to internal heat generation g per unit volume is given in equation (3.1). (Turgut, 2004)

$$\rho c \frac{\partial T}{\partial t} = \frac{\partial}{\partial x} \left(k \cdot \frac{\partial T}{\partial x} \right) + g \quad (3.1)$$

ρ (kg/m^3), c (kJ/kgK), T (K), k (W/mK), g (W/m^3), t (s), x (m) are respectively density, specific heat, temperature, thermal conductivity, heat generation per volume, time, thickness of the sample.

$\frac{\partial T}{\partial t} = 0$, under steady state conditions. If there is no heat generation then g becomes zero. The solution of the steady state problem is dependent on the boundary conditions. For unsteady state problems, since the temperature changes by time the solution depends on the initial condition.

Basicly we can define thermal conductivity from the Fourier-Biot heat conduction law as:

$$k = \frac{Q/A}{\Delta T/\Delta L} \quad (3.2)$$

where Q is the amount of heat passing through a cross section, A , and causing a temperature difference, ΔT , over a distance of ΔL . Q/A is therefore the heat flux which is causing the thermal gradient, $\Delta T/\Delta L$. (Turgut, 2004)

The measurement of thermal conductivity always involves the measurement of the heat flux and temperature difference. (Figure 3.1) The difficulty of the measurement is always associated with the heat flux measurement. Where the measurement of the heat flux is done directly (for example, by measuring the electrical power going into the heater), the measurement is called absolute. Where the flux measurement is done indirectly (by comparison), the method is called comparative. These two main methods are steady state other secondary methods are transient. (Principal methods of thermal conductivity measurements)

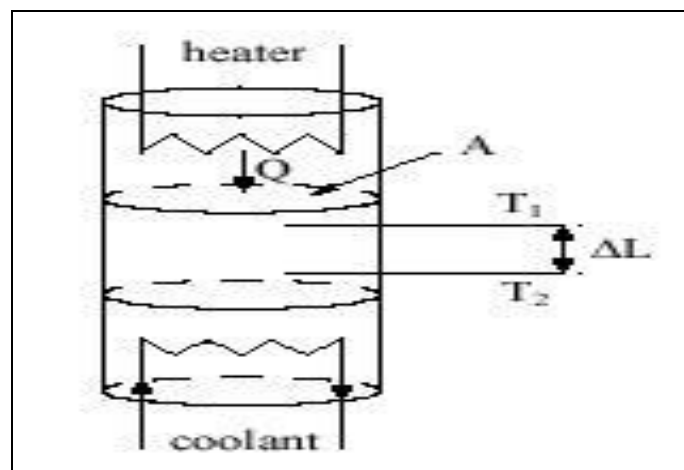


Figure 3.1 A heat conduction system. (Principal methods of thermal cond. measurements)

3.2 Thermal Conductivity Measuring Methods

3.2.1 Steady State Methods

Equation (3.1)'s modified forms can be used for one dimensional steady heat flow through plate, cylinder, and sphere.

3.2.1.1 Guarded Hot Plate

This is the most widely used method for the measurement of thermal conductivity of materials which are having low conductivity. It is suitable for dry homogeneous samples in slab forms. Heat flow is steady-state unidirectional. Its details are given by American Society for Testing Materials (ASTM) Standard ASTM 1955 and after then C 177-85 ASTM 1985. In this method, the heat source, the sample and the heat sink are placed in contact with each other and heated electrically with a thermal guard. The thermal guard plates are maintained at the same temperature as the adjacent surfaces, so that ideally no heat leakage occurs from source, sample or sink boundaries. It is assumed that the measured heat input to the specimen is all transferred across the sample. The thermal conductivity is computed by measuring the amount of heat input required to maintain the steady-state temperature profile across the test specimen (Figure 3.2). Since steady state conditions may take several hours to develop, this method is unsuitable to use with material in which moisture migration may take place. The method has been used for measuring the thermal conductivity of dried foods. (Turgut, 2004)

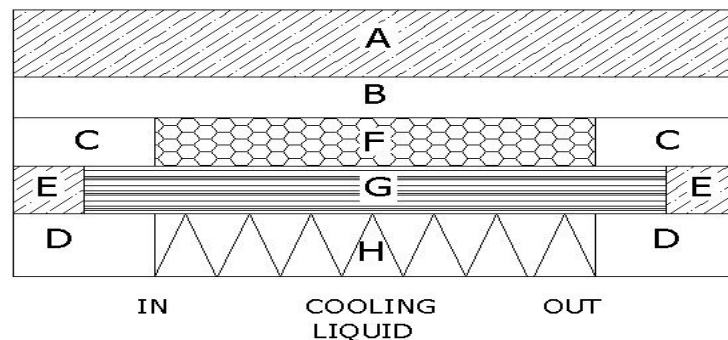


Figure 3.2 Single sample parallel plate method (A,E: insulation; B,C,D: guard heater; F: main heater; G: sample; H: cooling liquid). (Turgut, 2004)

3.2.1.2 Concentric Cylinder

Whereas the guarded hot plate is generally used for measuring the thermal conductivity of samples that can be formed into a slab, radial heat flow steady state methods are more commonly used with powdered or granular material.

A hollow cylindrical test device inner radius r_1 and outside radius r_2 , employs a central line (or cylindrical) heat source that has radial heat flux Q per unit length across the annulus can be measured by measuring the inside and outside temperatures T_1 and T_2 .

$$Q = \frac{2\pi k(T_1 - T_2)}{\ln(r_2/r_1)} \quad (3.3)$$

End effects are assumed negligible due to either the large length to diameter ratio of the test apparatus or the use of end guard heaters. After steady state has been established, the thermal conductivity can be calculated from the heating power, the length of the cylinder, the temperature differential between two internally (to the medium) located sensors and their radial position. Alternatively, the cylindrical sample can be bordered by the heater on one side and a reference material on the other side. Temperatures on all surfaces are monitored. The thermal conductivity of the test material is calculated from the temperatures, the radial position of the sensors and the thermal conductivity of the reference material. (Turgut, 2004)

3.2.1.3 Concentric Sphere

The specimen completely encloses the heating source in this method, eliminating end losses. Assuming that the surface of the central heater at a distance r_1 and the outer specimen surface at distance r_2 reach at the same temperature after the steady state has been established, heat flow will essentially be radial and the following equation can be used to determine thermal conductivity;

$$Q = \frac{4\pi k(T_1 - T_2)r_1 r_2}{\ln(r_2 - r_1)} \quad (3.4)$$

Because of practical difficulties, the method has not become popular. (Turgut, 2004)

3.2.2 Transient State Methods

The procedure for determining thermal conductivity in this method is to apply a constant heat flux to the sample, which must be in thermal equilibrium initially and to measure the temperature rise at some points in the specimen resulting from this applied heat flux. This method uses either a line heat source or one or more plane sources of heat. This is more appropriate for high moisture content materials because of the possibility of moisture migration during heating. The main advantages of the methods are that rapid results are possible, no heat flow measurements are required in many cases and a small temperature differential is acceptable. (Turgut, 2004)

3.2.2.1 Fitch Method

In 1935 Fitch developed a method for determining thermal conductivity. The main advantage of the method is simple determination and short time duration. The method consist of a heat source or sink in the form of a vessel filled with a constant temperature liquid and a sink or source in the form of a copper plug insulated all sides but one. (Figure 3.3) The sample is sandwiched between the vessel and the open face of the plug. (Turgut, 2004)

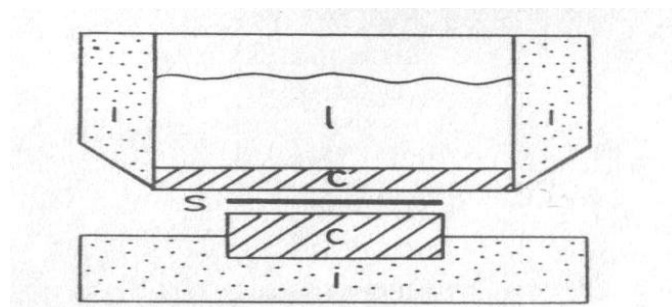


Figure 3.3 Fitch apparatus (C: copper plug; i: insulation; l: liquid; s: sample). (Turgut, 2004)

3.2.2.2 Probe Method

The non-steady state line heat source (hot wire) method and the probe method for measurement of thermal conductivity are based on a very similar theory. Both

methods have been used to measure thermal conductivity of biological materials, insulations, rocks, ceramics, foods, soils and glass over a wide range of temperatures and other environmental conditions. The line heat source method was suggested by Schleiermacher in 1888 and later by Stalhane & Pyk in 1931. Van der Held & Van Drunen used the method practically in 1949 for measuring the thermal conductivity of liquids. The line heat source method is more simple in analytical and experimental than the probe method, but it is relatively feeble and not useful for acute environmental conditions and field measurements. (Turgut, 2004)

3.2.2.3 3- ω Method

The 3- ω method has been used extensively for measuring the thermal conductivity of thin films and bulk materials. In this method a thin electrically conductive wire is deposited onto the specimen whose thermal conductivity needs to be measured. The wire functions as both a heater and a temperature sensor. An ac current with angular modulation frequency ω is driven through the wire, causing Joule heating at a frequency of 2ω . The generated thermal wave diffuses into the specimen and the penetration depth is determined by the thermal diffusivity of the specimen and the frequency of the ac current. Since the resistance of the heater is proportional to the temperature, the resistance will be modulated at 2ω . The voltage drop along the wire thus contains a third harmonic that depends on the ac temperature rise of the heater and could be used to extract the thermal conductivity of the specimen. Thermal conductivities of thin films down to several nanometers thickness were measured using this technique. Moreover, the 3- ω method was employed to measure the thermal conductivity of anisotropic thin films. For anisotropic thermal conductivity measurements, the combination between the heater wire width and the film thickness determine the measurement sensitivity to the in-plane and cross-plane thermal properties of the film. Choosing the heater width much larger than the film thickness, the measured temperature drop could be assumed to be sensitive mainly to the crossplane thermal conductivity of the film. If the wire width is smaller or comparable to the film thickness, the heat produced in the heater wire

tends to spread inside the film and measured temperature signal is influenced by both the in-plane and cross-plane thermal conductivities of the film. (Turgut, 2004)

3.2.2.4 Laser Flash method

The flash method is the most frequently used technique to measure thermal diffusivity for moderate to good thermal conducting materials (approximately > 0.5 W/m K) in the perpendicular to surface direction. Plane measurements can be made using modifications of the method involving a “point” energy source and radial temperature measurements across the back surface. The basic method is based on a measurement of the temperature rise on the back face of a thin disc sample caused by a short energy pulse on the front surface.

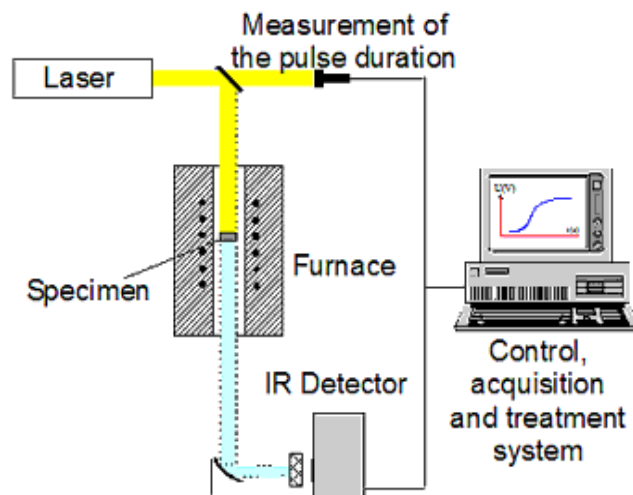


Figure 3.4 Schematic of a typical flash method system.

(Laser flash method)

The specimen is placed in a furnace and heated to a uniform temperature. A short (1 ms or less) pulse coming from a laser or a flash lamp irradiates one surface of the specimen. The resulting temperature rise on the rear surface (and/or the front surface in some cases) is measured either with a fixed thermocouple or more usually by an IR detector (HgCdTe, InSb or other depending on the temperature range). (Figure 3.4) The thermal diffusivity is calculated from this temperature versus time curve and the thickness of the sample. Knowledge of the energy absorbed and the specimen

emissivity are not needed. The specimen holder is designed to minimise thermal contact with the specimen and to suppress stray light transmitted from the laser beam to the IR detector. Both sides of the specimen should be coated with a thin layer of graphite or other high emissivity material to both optimise absorption of the energy pulse and emission of thermal radiation. (Laser flash method)

For *thermal conductivity measurements*, there are steady-state methods (up to 1200 K) and transient methods (in particular over 1500 K). If the material under test is a conductor the specimen can be self-heated by passage of an electric current. As a consequence of the wide ranges of thermal property there is no single method of measurement that can be used for measurement of either property, in particular thermal conductivity. To obtain acceptable values for the measured property, the material type and its range of property value over its operational temperature range will influence particularly the type of method used and the size and conjunction of the test specimen and apparatus. (Thermal conductivity measurement methods)

Table 3.1 Common thermal conductivity or thermal diffusivity measurement methods (Thermal conductivity measurement methods)

| Measurement method | Short description | Material type | T range in °C | Property range in W/(m.K) |
|--------------------------|---|--|---------------|---------------------------|
| Comparative technique | A secondary method of thermal conductivity measurement in which steady-state linear heat flow is established in a stack consisting of a specimen sandwiched between two references and surrounded by a cylindrical guard heater | all solids | 0 to 1000 | 0.2 to 200 |
| Four-probe technique | Thermal conductivity is determined from measurement of the electric resistivity; current and voltage are normally measured with four probes | metals and metallic alloys | 20 to 1600 | 10 to 800 |
| Guarded heat flow method | Similar in principle to the heat flow meter method but used to measure much smaller higher conductivity specimens using different calibration materials and cylindrical guard around the test stack | polymers, rocks, ceramics, foods, some metals and alloys | 100 to 300 | 0.2 to 20 |
| Guarded hot-plate | Steady-state linear heat flow established in a large flat sample (usually in two nominally identical pieces) sandwiched between a controlled and guarded central hot plate and cold plates operating at a controlled lower temperature. A well-established absolute | solid, opaque, homogeneous, composites, insulation materials | -180 to 1000 | 0.0001 to 2 |

Table 3.1 (Continued)

| | | | | |
|--|---|--|--------------|---|
| | technique having high accuracy, especially at ambient temperatures. | | | |
| Heat-flow meter method | A secondary steady-state method using a similar configuration to the guarded hot plate but normally using one large self-guarding specimen in conjunction with a heat flux transducer and with the apparatus calibrated with one or more reference materials or transfer standards | insulation materials | -100 to 200 | 0.007 to 1.0 |
| Hot-box apparatus, either guarded or calibrated (thermal resistance) | Not generally used for materials but for measuring the steady-state thermal transmission properties (U-value) or the thermal conductance of building envelope components and systems. A large specimen is placed between a hot and a cold chamber operating at fixed temperatures, humidity and air flow conditions. A guarded metering box is attached to the central section of the specimen in the guarded hot box while in the calibrated version a well insulated much larger box is calibrated with a transfer Standard | systems containing insulation, wood, masonry, glass and other materials and products used for the building envelope | -20 to 40 | 0.2 to 5 |
| Hot strip method | Very similar in principle to the hot wire method but uses a narrow thin metal foil pressed directly between two specimen pieces as the power source | glasses, foods ceramics, etc | -50 to 500 | 0.1 to 5 |
| Hot wire method | Three forms available, either a single or crossed resistive wire or two parallel wires a small distance apart. A quasi-steady state method where the thermal properties are obtained from the temperature v. time response due to a heat flux generated by the wire embedded in the specimen. The curve is analysed in accordance with a model based on a solution of the time-dependent heat equation under a particular set of boundary conditions. In principle an absolute method | refractory materials, many solid types including earth minerals, glasses, plastics granules and powders, plus fluids and gases | -40 to 1600 | 0.001 to 20 |
| Laser flash method | Thermal diffusivity is determined from an analysis of the temperature rise v. time response induced by absorption of a pulse of laser energy | metals, polymers, ceramics | -100 to 3000 | 0.1 to 1500 |
| Angstrom method | A long thin (0.3 - 0.9 mm diameter, 100 - 300 mm long) radiating rod, tube or bar of a good conducting material, assumed to behave as a semi-infinite medium, is heated at one end by a sinusoidal heat source with a period of typically 100 to 150 s. Temperature sensors are attached at two or more positions along the rod axis. Thermal diffusivity is determined from the resulting velocity and amplitude decrease using one of a number of solutions to the mathematical model. | Metals, alloys, graphite, ceramics | 25 to 1300 | above 0.5 |
| Modified Angstrom method | The partially masked blackened surface of a thin rectangular specimen is irradiated by uniform chopped light at fixed frequencies and the ac temperature excursion on the opposite face monitored as the specimen is moved in small increments. The in-plane thermal diffusivity is then determined from the linear amplitude decay and phase shift | diamond, metals, semiconductors, ceramics and polymer multi-layered composites | -100 to 500 | Covers a range of six orders of magnitude |

Table 3.1 (Continued)

| | | | | |
|---|--|---|-------------|--|
| | curves | | | |
| Modulated beam technique | Thermal diffusivity is determined from the temperature modulation induced by absorption of the modulated light beam from a xenon lamp or other source | metals, polymers, ceramics | 300 to 2000 | 1 to 500 |
| Needle probe | A modification of the hot wire technique whereby the heat source and temperature measurement sensor(s) are together sealed into a long thin tube which is then directly embedded in the specimen or fixed in grooves cut across the matching surfaces of two specimen pieces. Can be used for in-situ measurements. Some versions use reference materials for calibration although in principle the technique is an absolute one | soils, minerals, solid and molten polymers and foods, rubber, particulates, powders | -50 to 500 | 0.05 to 20 |
| Photothermal methods | Intensity modulated light is directed onto the specimen surface and the run-time behaviour of the resultant thermal waves is detected. The amplitude and phase change are evaluated as a function of the modulation frequency using appropriate models to obtain the thermal diffusivity or thermal conductivity | small specimens of most solid material types | -50 to 500 | 0.1 to 200. Methods also very useful in a qualitative NDT mode |
| Pipe test method (radial flow) | Similar in principle to the guarded hot plate but using a long cylinder or tubular specimen wrapped around a central heater with end guard heaters and employing radial heat flow to measure thermal conductivity and thermal transference | insulation such as calcium silicates, mineral and refractory fibre blankets, cellular plastics, foamed glass, microporous block and powder products | 50 to 800 | 0.02 to 2, depending on material type and temperature |
| Contact transient methods - Plane source with pulse transient | Multi-property version of contact transient. A heat pulse generated during an appropriate time through a metal foil on one face of the specimen and the temperature response measured by a sensor attached to the other specimen surface | polymers, rocks, ceramics, some alloys, thermal insulations, liquid samples such as water, oils, molten polymers | -40 to 400 | 0.05 to 50 |
| Contact transient methods - Plane source with step-wise transient | Similar to the pulse transient with a heat flux generated for an appropriate time | soils, minerals, solid and molten polymers and foods, rubber, particulates, powders, some building materials | -40 to 400 | 0.05 to 50 |
| Subsecond techniques | Thermal conductivity is determined from the power balance obtained during the cooling part of the rapid heating and cooling of a thin wire. The heat dissipated by the specimen is lost by radiation and conduction | electrical conductors only | 700 to 3300 | 50 to 400 |

3.2.2.5 Hot-Disk Method

The present rapid development of new materials for physical, chemical, biological and medical applications has resulted in increased requirements for reliable thermal

performance data. Established methods for obtaining such data often require large samples and time consuming procedures. With this background in mind efforts have been made to develop alternative methods to cover as wide a range of materials as possible. Some of these new methods are referred to as contact transient methods (CTM) and they often present a possibility of measuring both the thermal conductivity and the thermal diffusivity of the materials in question. With these methods it is at present possible to study a variety of materials like: metals, alloys, ceramics, glasses, polymers, composites, powders and liquids. Besides covering this broad range of dense, homogeneous and isotropic materials, some of these methods can be used to measure properties of anisotropic materials. An added advantage is the ability to cover quite a large temperature range and also work at different pressures. In the present the transient hot strip (THS) and the transient plane source (TPS) or hot disk methods are used. It is referred to as "The Gustafsson Probe" in honor of its inventor. (Hot-Disk method)

The encapsulated Ni-spiral sensor is sandwiched between two halves of the sample (solid samples), or embedded in the sample (powders, liquids). During a pre-set time, 200 resistance recordings are taken and from these, the relation between temperature and time is established. A few parameters, like the "Output of Power" to increase the temperature of the spiral, the "Measuring Time" for recording 200 point and the size of the sensor are used to optimise the settings for the experiment so that thermal conductivities from 0.005 W/mK to 500 W/mK can be measured.

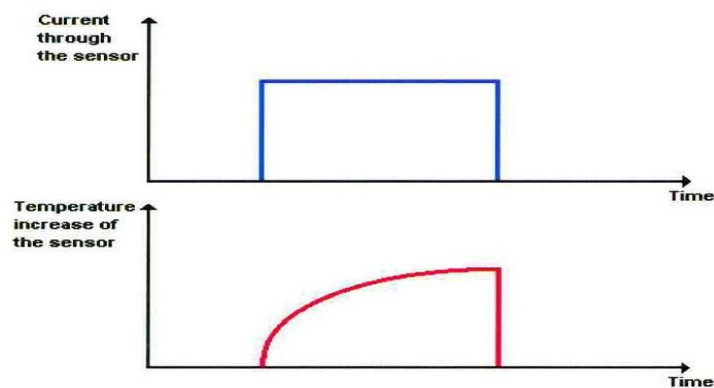


Figure 3.5 Transient recording of the thermal transport properties of the material surrounding the sensor. (Instruction manual of the Hot-Disk software)

Measurements on standart materials ranging from Polystyrene to Aluminum metal show that the accuracy over the whole range of thermal conductivities is within +/- 5% and the reproducibility is within +/-2% cf.

In order to obtain a reasonably high initial resistance of the sensor element and the same time be able to work with a convenient and compact configuration of the sample, the Hot Disk sensor has been designed in the form of a double spiral to minimise the total size of the sample. To theoretically describe how the Hot Disk behaves, the thermal conductivity equation has been solved assuming that the Hot Disk consists of a certain number of concentric ring heat sources located in an infinitely large sample. If the Hot Disk is electrically heated, the resistance increase as a function of time can be given as:

$$R(t) = R_0 \{1 + \alpha [\Delta T_i + \Delta T_{ave}(\tau)]\} \quad (3.5)$$

R_0 is the resistance of the disk just before it is being heated or time $t = 0$, α is the Temperature Coefficient of the Resistivity (TCR), ΔT_i is the constant temperature difference that develops almost momentarily over the thin insulating layers which are covering the two sides of the Hot Disk sensor material (Nickel) and which make the Hot Disk a convenient sensor. $\Delta T_{ave}(\tau)$ is the temperature increase of the sample surface on the other side of the insulating layer and facing the Hot Disk sensor (double spiral). (Instruction manual of the Hot-Disk software)

From equation (3.5) we get the temperature increase recorded by the sensor:

$$\Delta T_{ave}(\tau) + \Delta T_i = (1/\alpha) \cdot ((R(t)/R_0) - 1) \quad (3.6)$$

Here ΔT_i is a measure of the “thermal contact” between the sensor and the sample surface with $\Delta T_i = 0$ representing perfect “thermal contact” closely realised by a deposited (PVD or CVD) thin film or an electrically insulating sample.

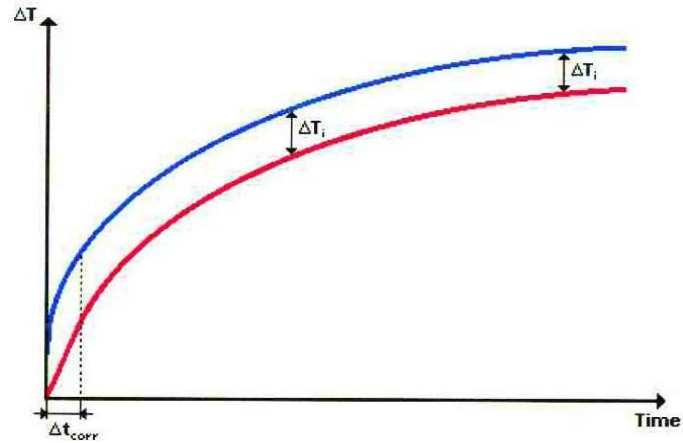


Figure 3.6 The blue curve indicates the temperature increase of the sensor itself and the red one shows how the temperature of the sample surface is increasing. (Instruction manual of the Hot-Disk software)

ΔT_i becomes constant after a very short time ΔT_i which can be estimated as:

$$\Delta T_i = \frac{\delta^2}{\kappa_i} \quad (3.6)$$

where δ is the thickness of the insulating layer and κ_i is the thermal diffusivity of the layer material. (Figure 3.6)

The time dependent temperature increase is given by the theory as:

$$\Delta T_{ave}(\tau) = \frac{P_o}{\pi^{3/2} \cdot a \cdot \Lambda} \cdot D(\tau) \quad (3.7)$$

where P_o is the total output of power from the sensor during the transient recording, a is the overall radius of the disk, Λ is the thermal conductivity of the sample that is being tested and $D(\tau)$ is a dimensionless time dependent function with:

$$\tau = \sqrt{\frac{t}{\Theta}} \quad (3.8)$$

In this equation t is the time measured from the start of the transient recording. Θ is the characteristic time defined as:

$$\Theta = \frac{a^2}{\kappa} \quad (3.9)$$

where κ is the thermal diffusivity of the sample.

Now by making a computational plot of the recorded temperature increase versus $D(\tau)$, we get a straight line, the intercept of which is ΔT_i and the slope is

$$\frac{P_o}{\pi^{3/2} \cdot \alpha \cdot \Lambda}$$

using experimental times much longer than Δt_i .

Since κ and by that Θ are not known before the experiment, the final straight line from which the thermal conductivity is calculated, is obtained through a process of iteration. In this way it is possible to determine both the thermal conductivity and the thermal diffusivity from one single transient recording. (Instruction manual of the Hot-Disk software)

When the Hot Disk method is compared with older Hot Wire and Guarded Hot Plate techniques of thermal conductivity measurement, both require considerably larger samples and The Guarded Hot Plate method necessitates a temperature gradient slowly forming across the sample but the Hot Disk method furnishes direct and instant measurement of how the heat generated by the sensor propagates into the material. Static methods such as the Guarded Hot Plate are inevitably affected by contact resistance, which causes inherent error as it builds up between the thermocouple and sample surface. Static methods cannot compensate for this, and a negative influence is unavoidable even at conductivity levels as low as 1-2 W/mK. The Hot Disk method employs data stemming from heat propagation in undisturbed material for its calculations and its results hence represent the bulk properties of the material. (Hot-Disk method)

CHAPTER FOUR

MATERIALS AND METHODS

4.1 Materials and Methods

4.1.1 HDPE/Graphite

The matrix material (fabricated in Petkim Petrokimya Holding A.Ş.) is a high-density polyethylene in powder form (commercial name: Petilen I 668 (UV)), with a density of 0.966-0.970 g/cm³ at 23°C and a melt flow rate is 4.4-6.5g/10 min (at 190°C, 2.16 kg). The metallic filler is graphite powder (produced in NanoAmor, particle size 400 nm) with a density of 2.25 g/cm³ at 20°C.

HDPE is produced by catalytic polymerisation of ethylene in either slurry (suspension), solution or gas phase reactors. The choice of catalyst and/or the use of bimodal processes are used to modulate the quality of the output. HDPE is a thermosetting white solid whose molecular chains are comparatively straight and closely aligned. (Figure 4.1) It is resistant to most chemicals, insoluble in organic solvents and has high impact and tensile strength. HDPE is the third largest commodity thermoplastic. A major outlet for HDPE is in blow-moulding applications such as bottles, packaging containers, drums, fuel tanks for automobiles, toys and house wares. Injection-moulded articles made from HDPE include crates, pallets, packaging containers and caps, paint cans, house wares and toys. Global demand has been reasonably strong and growing ahead in most countries. Future global growth is expected to be around 5%/year. (Polyethylene - high density (HDPE))

Table 4.1 Properties of polymer matrix, HDPE (Petkim)

| Property | Unit | Value | Test Method |
|--|--------------------|--------------|--------------------|
| <i>Melt Flow Rate (2160g, 190°C)</i> | g/10 min | 4.4-6.5 | ASTM D-1238 |
| <i>Density, 23°C</i> | g/cm ³ | 0.966-0.970 | ASTM D-1505 |
| <i>Tensile Strength</i> | | | |
| - <i>At Yield</i> | Kg/cm ² | 295 | ASTM D-638 |
| - <i>At Break</i> | Kg/cm ² | 240 | ASTM D-638 |
| - <i>Elongation At Break</i> | % | 1250 | ASTM D-638 |
| <i>Stiffness</i> | Kg/cm ² | 10450 | ASTM D-747 |
| <i>Izod Impact Strength</i> | Kg cm/cm | 5 | ASTM D-256 |
| <i>ESCR, (F50)</i> | Hour | 4 | ASTM D-1693 |

Graphite is one of the natural crystalline allotropic form of carbon, the other one is diamond. Each has its own distinct crystal structure and properties. Graphite is generally greyish-black, opaque and has a lustrous black sheen. (Figure 4.1) It is unique in that it has properties of both a metal and a non-metal. It is flexible but not elastic, has a high thermal and electrical conductivity, and is highly refractory and chemically inert. It has a low adsorption of X-rays and neutrons making it a particularly useful material in nuclear applications. (Graphite's properties)

There are two main classifications of graphite, natural and synthetic. Natural graphite is a mineral consisting of graphitic carbon. It varies considerably in crystallinity. It is subdivided into three types; amorphous, flake and high crystalline. Synthetic graphite can be produced from coke and pitch. It tends to be of higher purity though not as crystalline as natural graphite. Natural graphite has applications in metallurgy, pencil production, refractories, coatings, lubricants, paint production, making batteries, grinding wheels, powder metallurgy, secondary steel making and fabrication of graphite foil. Synthetic graphites are used in aerospace applications, batteries, carbon brushes, graphite electrodes for electric arc furnaces for

metallurgical processing and moderator rods in nuclear power plant. (Graphite's properties)

Table 4.2 Physical and chemical properties of graphite (Graphite powder)

| Physical and Chemical Properties | Graphite (natural) powder (400 nm) |
|--|---|
| Bulk Density (g/cm ³) | 0.03-0.035 |
| Purity (%) | 99.9 (metal base) |
| Impurities | (quartz+mica)<0.1%,H ₂ O~0.2%, |
| pH | 6-7 |
| Particle morphology | Flaky |
| Color | Black |
| Melting point (°C) | 3652-3697 |
| Odor/Water | Odorless/Insoluble |
| Density (at 20°C) (g/cm ³) | 2.25 |



Figure 4.1 Graphite-HDPE and their chemical formulas. (image above is from Nanoage)

In different weight contents (4, 6, 8, 10, 12, 15, 20, 30 %) of graphite/HDPE nanocomposites were produced. Firstly, graphite was dried at 120°C for 6 hours. Samples are prepared by the mold compression process. HDPE and graphite powders are mixed in a Brabender Plasticorder W30 internal mixer at 180°C for a total mixing time of 10 min, the mixing chamber capacity is 30 ml. (Figure 4.2) The rotors were turned at 35 rpm for 15 minutes at 180°C. The mixed powder was then melted under pressure in a mold and solidified by aircooling. The process conditions were molding temperature of 180°C and pressure of 40kPa for 1 minute. The resulting samples for

thermal conductivity measurements are circular in shape of 15 mm diameter and 10 mm thickness because of the measuring probe.



Figure 4.2 General view Brabender Plasticorder W30/The mixing chamber and the rotors after the mixing process of the composite. (Tavman et al., 2008)

4.1.2 Measurement Method and Apparatus

With the TPS technique, the probe comprises a flat sensor with a continuous double-spiral of electrically-conducting Nickel (Ni) metal etched out of thin foil and sandwiched between two layers of Kapton. Although only 0.013 to 0.025 mm thick, the Kapton provides both electrical insulation from the sample and mechanical stability for the probe. The sensor is normally placed between the surfaces of two pieces of the sample to be measured. Different sizes and formats of sensor are available to accommodate a large variety of samples. (Hot-Disk method)

During measurement, a current passes through the Nickel spiral and creates an increase in temperature. The heat generated dissipates through the sample on either side at a rate dependent on the thermal transport characteristics of the material. By recording the temperature versus time response in the sensor, these characteristics can accurately be calculated. (Hot-Disk method)

As the Hot Disk probe constitutes both heat source and temperature sensor, it allows at once quick, convenient, and reliable experimental results.

The THS method is based on the use of an evaporated strip or a metal foil for simultaneously heating and recording the temperature increase of the sample. The strips can be made of different materials. However, preference should be given to materials or thin films having as high a temperature coefficient of the electrical resistivity (TCR) as possible. The TPS method is based on the use of an electrically insulated sensor, which is designed as a bifilar spiral etched out of a 10 μm thick metal foil and covered on both sides by thin dielectric insulating films. Thus far Nickel or Molybdenum has been used as heater / temperature sensing material due to their rather high TCR and in most cases a polyimide (Kapton) or a mica material has been used as insulating films. The principle of measurement with these methods is to generate a heat pulse for a given time by passage of an electrical current through the combined heater/temperature sensing probe. The resulting temperature increase is then analysed in accordance with the solution of the thermal conductivity equation, using initial and boundary conditions corresponding to the experimental set up. With both these methods it is under certain experimental conditions possible to obtain both the thermal conductivity and the thermal diffusivity from one single recording. The thermal conductivities covered to date range from 0.005 to 500 W/mK over temperatures from 50 K to 1800K and with careful selection of sample size, sensor design, output of power and transient time a comparably high precision in the thermal conductivity measurements is easily reached. (Hot-Disk)

The method uses a sensor element with an engraved pattern of a thin double spiral. The spiral is made of Ni metal and has specific electrical resistivity properties. The spiral is embedded between two layers of Kapton, to give it mechanical strength and electrical insulation. Thus measurements can also be performed in electrically conductive materials. The total thickness of the sensor is 0.65 mm and for this specific application the diameter was 20 mm. The probing depth in a transient experiment should be of the same order as the diameter of the hot disk. To achieve this for different materials and sample-sizes, measurement-times and sensor size can

be varied. (Comparison of Thermal Properties)

Measurements are performed by placing the sensor between two samples of the same material. The surfaces of the samples have to be fairly smooth and reasonably flat in order to limit the contact resistance between the sensor and the sample surfaces. During the measurement, the sensor acts both as a heat generator of a heat pulse and as sensor for the temperature response. The temperature vs. time response is measured in 200 data points. (Comparison of Thermal Properties)

The evaluation uses the fact that the electrical resistance for a thin Ni spiral at any time is a function of its initial resistance, the temperature increase and the temperature coefficient of the resistivity. A model of heat propagation through the sample, assuming a plane source (sensor) and an infinite sample in perfect contact with the sensor surfaces is stored in the software. By fitting measured temperatures to this model, through a number of iterations, the thermal diffusivity and thermal conductivity are determined. (Comparison of Thermal Properties)

4.1.3 Experimental Set-up

The surfaces of the samples have to be smooth and flat in order to limit the contact resistance between the sensor and the sample surfaces, so firstly, sample's surfaces are rubbed with a polishing machine. (Figure 4.3) Sensor was placed between samples. (Figure 4.4)

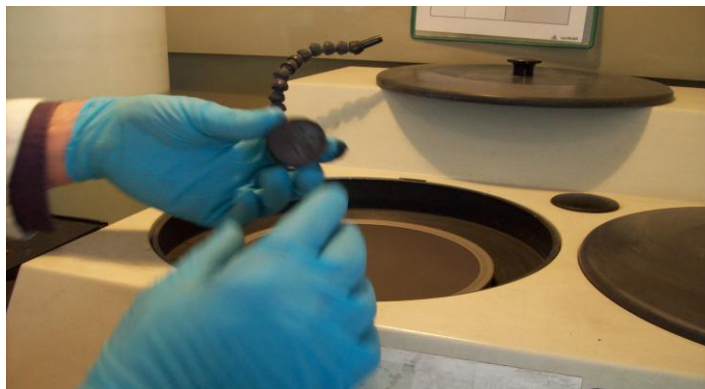


Figure 4.3 Polishing machine.



Figure 4.4 Different views of the experimental support.

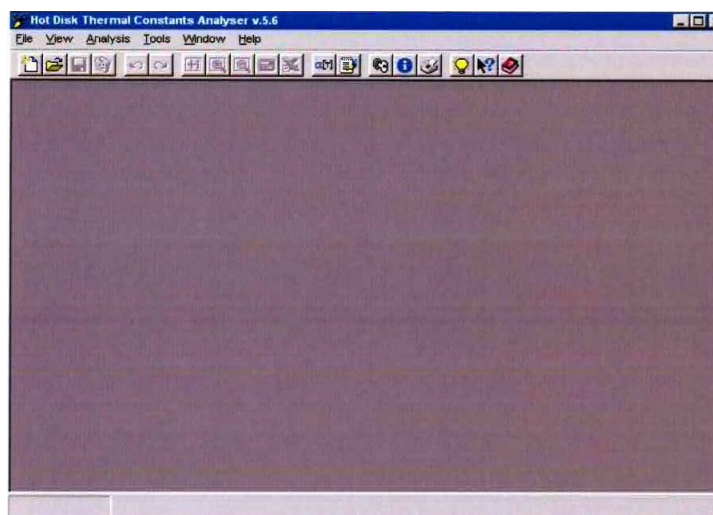


Figure 4.5a The main window of the Hot-Disk program

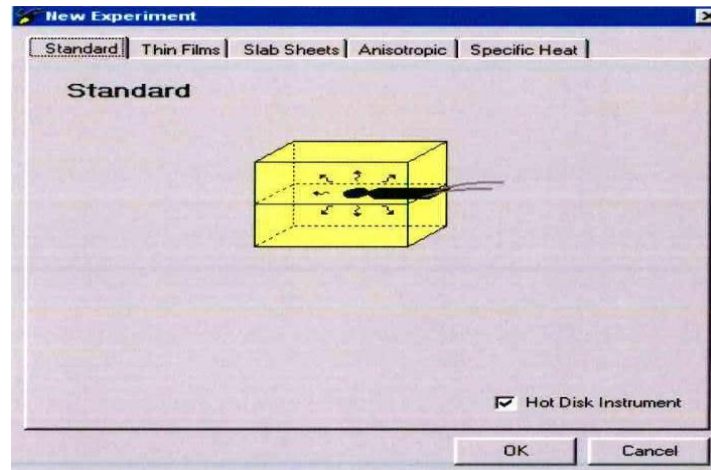


Figure 4.5b The experimental option window of the Hot-Disk Thermal Constants Analyser software.

The program “Hot Disk Thermal Constants Analyser v.5.9.4” is started. (Figure 4.5) From “Standart” buton, you open a new window. (Figure 4.6) You enter the available probing depth, initial temperature, disk type (kapton or mica), radius of disk, TCR (temperature coefficient of resistivity), measuring time and output power. (Instruction manual of the Hot-Disk software)

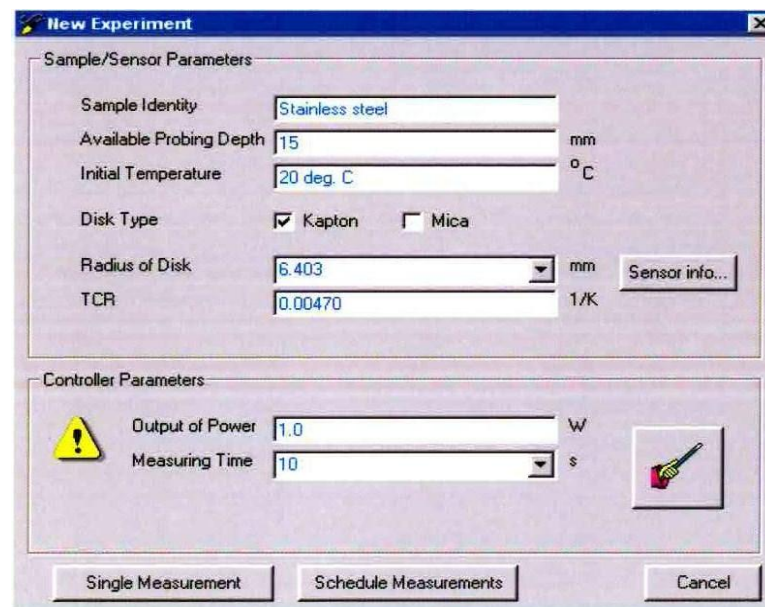


Figure 4.6 The standart-new experiment window.

Available probing depth is selected according to the size of the disk type and samples.

$$\Delta_p = 2.(\kappa.t_{\max})^{1/2}$$

κ , thermal diffusivity, t_{\max} , measuring time

| Temperature (°C) | TCR (1/K) |
|------------------|-----------|
| 0 | 0.00484 |
| 20 | 0.00470 |
| 30 | 0.00463 |
| 40 | 0.00456 |
| 50 | 0.00449 |
| 60 | 0.00443 |
| 70 | 0.00436 |
| 80 | 0.00430 |
| 90 | 0.00424 |
| 100 | 0.00418 |
| 110 | 0.00412 |
| 120 | 0.00406 |
| 150 | 0.00390 |
| 200 | 0.00368 |
| 300 | 0.00342 |
| 400 | 0.00149 |
| 500 | 0.000971 |
| 600 | 0.000860 |
| 700 | 0.000770 |
| 750 | 0.000735 |

Figure 4.7 Approximate TCR values for the Hot-Disk sensors.

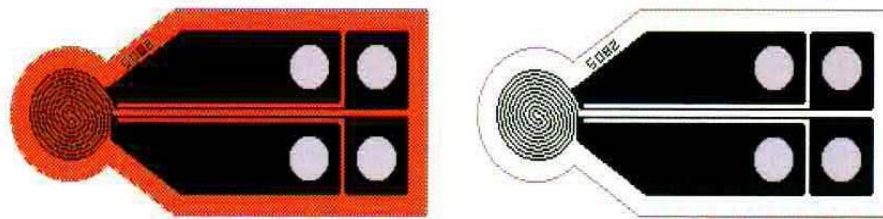


Figure 4.8 Hot-Disk sensors with kapton insulation(left) and mica insulation(right).

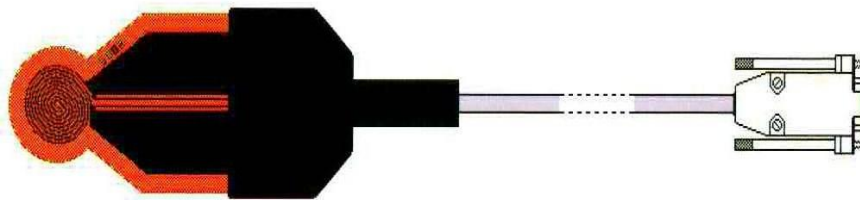


Figure 4.9 Kapton insulated Hot-Disk sensors with room temperature cable extension.

| Design | Radius [mm] | Kapton | Mica |
|--------|-------------|--------|------|
| 7531 | 0.526 | x | N/A |
| 7577 | 2.001 | x | N/A |
| 5465 | 3.189 | x | x |
| 5501 | 6.403 | x | N/A |
| 5082 | 6.631 | N/A | x |
| 4921 | 9.719 | x | x |
| 8563 | 9.868 | x | N/A |
| 4922 | 14.610 | x | x |
| 8562 | 14.725 | x | N/A |
| 5599 | 29.52 | x | x |

Figure 4.10 Available hot disk sensor radii.

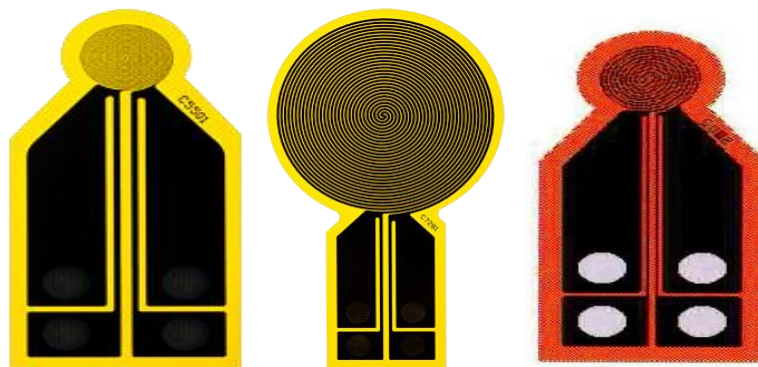


Figure 4.11 Hot-disk sensors (5501-7281-5082).

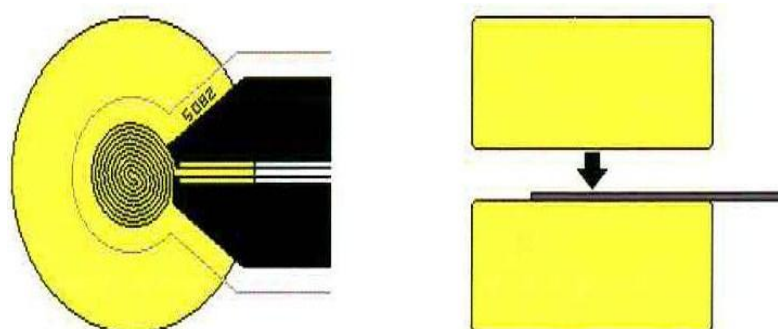


Figure 4.12 Sensor position between samples.

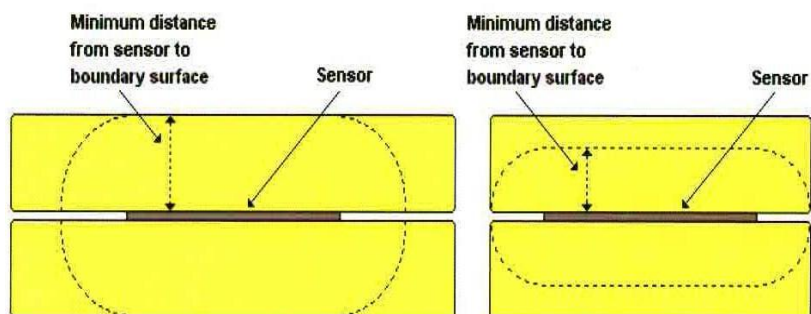


Figure 4.13 Minimum distance from sensor to boundary surface.

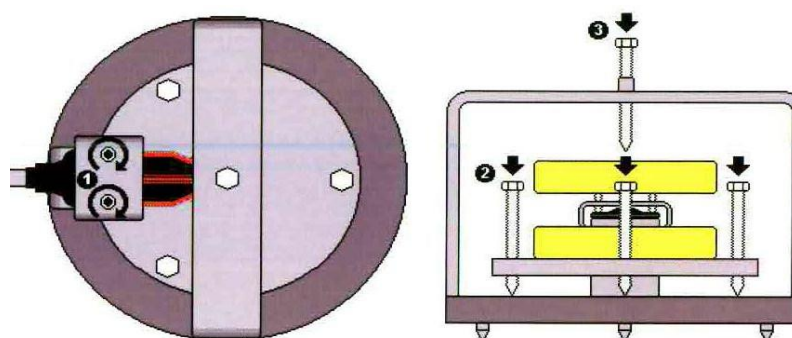


Figure 4.13 Room temperature sample support.

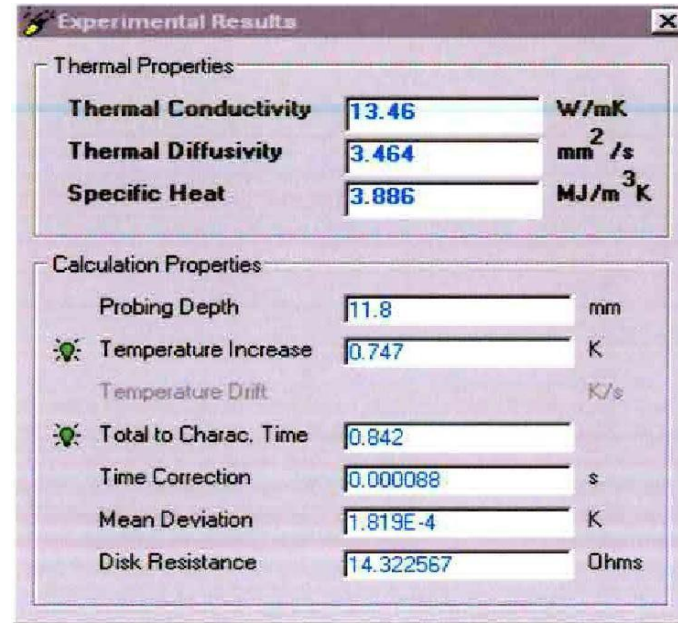


Figure 4.14 The experimental results window.

In the experimental results' window, you take care of temperature increase and total to characteristic time (it must be between 0.5-1.0), if the lights are green in the window, you don't need to repeat the experiment. (Figure 4.14)

Table 4.3 Standart Specifications for the "Hot Disk Thermal Constants Analyser v.5.9.4" program

| |
|---|
| Temperature Range: 30 K to 450 K using Kapton insulated Disk elements 400 K to 1000 K using Disk elements insulated with Mica. |
| Radius of Disk Spiral: To select Disk sensors for situations with different probing depths, several Disk elements are available, with radii from 0.492 mm to 29.40 mm. |
| Sensor Material: The double spiral is made of Nickel. |
| Sample Size: Depends on the diameter of the Disk elements and the material under study. Minumum size is a sample piece of diameter/thickness 1.5-2 mm. |
| Thermal Conductivity Range: 0.005 W/mK to 500 W/mK. |
| Reproducibility: Thermal conductivity +/-2%, thermal diffusivity +/-5%, specific heat (per unit Volume) +/-7%. |

CHAPTER FIVE

RESULTS AND DISCUSSION

Thermal conductivity of HDPE/graphite composites nonlinearly increases with the increasing volume content of graphite in the composite. This increase is seen deeply after 6% volume content of graphite. All theoretical models except Russell, until 6% volume content of graphite, fail to predict the experimental results. (Figure 5.1 and 5.2)

Distribution of the filler (graphite powder) in the matrix (HDPE) was investigated and the images were taken from electron scanning microscope at different magnifications in the volume contents of 2%, 5%, 10%, 16% graphite.

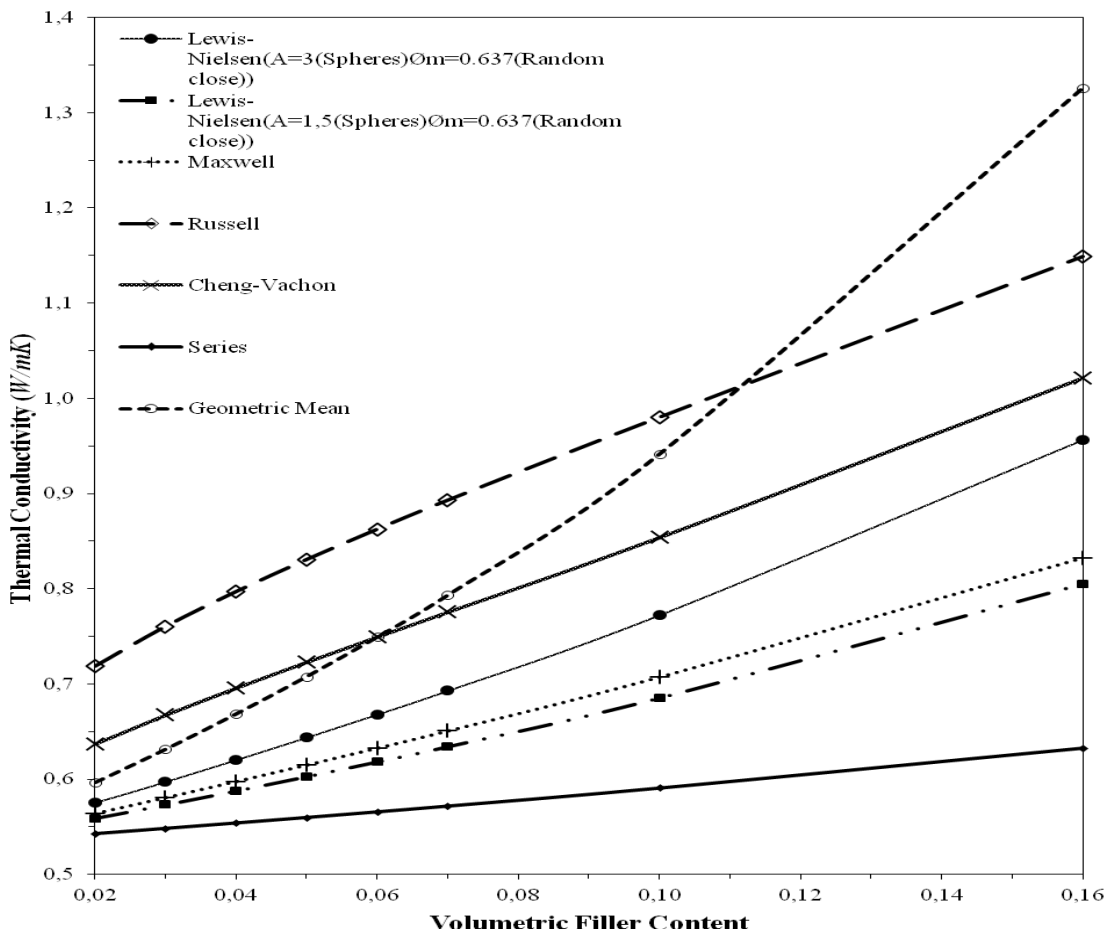


Figure 5.1 Thermal conductivity models of HDPE/graphite nanocomposites as a function of filler content.

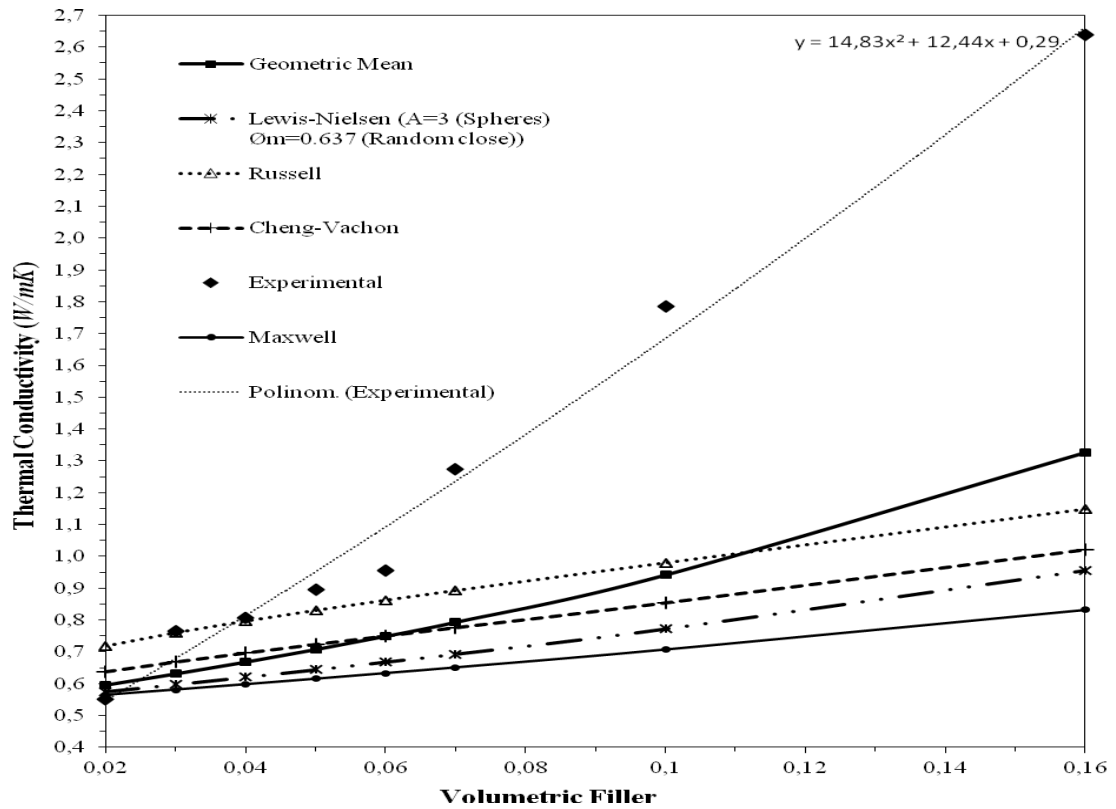


Figure 5.2 Thermal conductivity models of HDPE/graphite nanocomposites are comparing with experimental results.

Table 5.1 Weight and volume portions of graphite

| Weight content of graphite (%) | Volume content of graphite (%) | Thermal conductivity (W/mK) |
|--------------------------------|--------------------------------|-----------------------------|
| 4 | 2 | 0,55061 |
| 6 | 3 | 0,76608 |
| 8 | 4 | 0,80669 |
| 10 | 5 | 0,89571 |
| 12 | 6 | 0,95487 |
| 15 | 7 | 1,27264 |
| 20 | 10 | 1,78526 |
| 30 | 16 | 2,63906 |

To compute weight portion of the filler from the volume portion;

$$\varphi_v = \frac{\varphi_w * \rho_w}{\rho_p + \varphi_w * \rho_w - \varphi_w * \rho_p} \quad (5.1)$$

φ_v : volume content, φ_w : weight portion of the filler, ρ_p : density of the filler, ρ_w : density of the matrix (HDPE) (Zhang, Gu, Fujii, 2006) (in the formulas ρ_p : 2,16 g/cm³, ρ_w : 0,941 g/cm³ are used as in the literature)

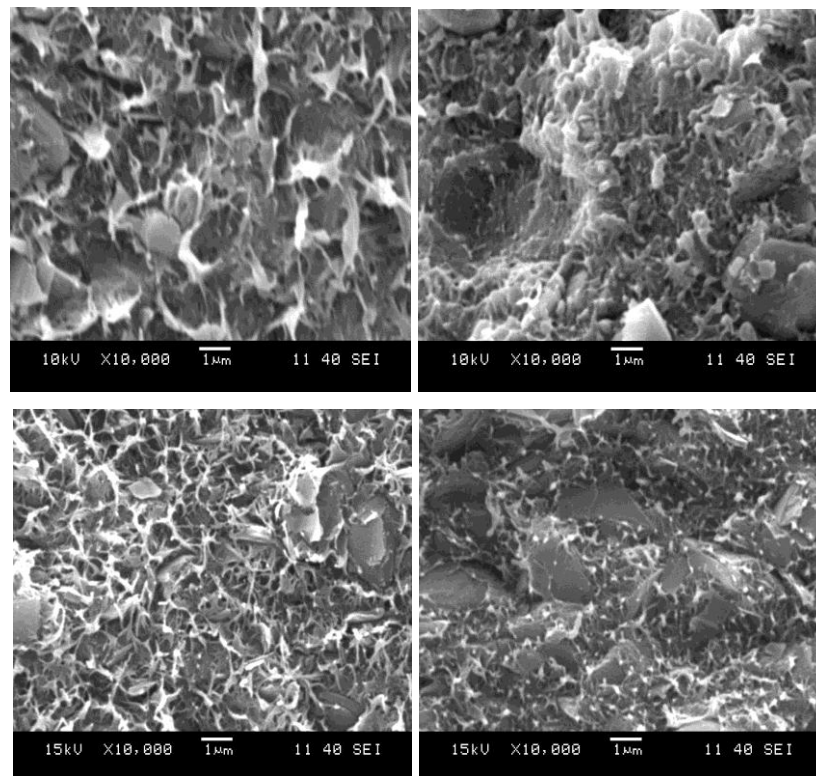


Figure 5.3 SEM images of HDPE/graphite, vol 2%, 5%, 10%, 16% graphite (magnification 10000x).

As seen from the SEM images (Figure 5.3-4-5-6-7), in the big magnification numbers, surface morphology of the composites is more definite. Decreasing values (5000x, 2000x, 1000x, 500x) of the magnifications make the images unclear, the details of composites can not be seen clearly. The images are taken from the samples containing 2, 5, 10, 16% volume fraction of graphite and with the increasing volumes of graphite, we can observe that graphite and HDPE were well-dispersed in the composite.

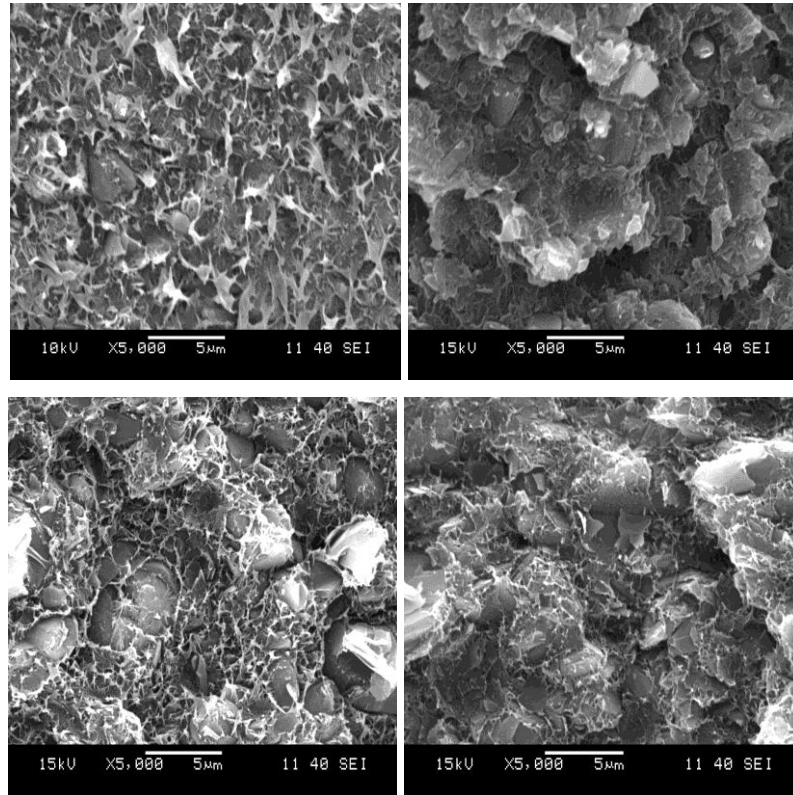


Figure 5.4 SEM images of HDPE/graphite, vol 2%, 5%, 10%, 16% graphite (magnification 5000x).

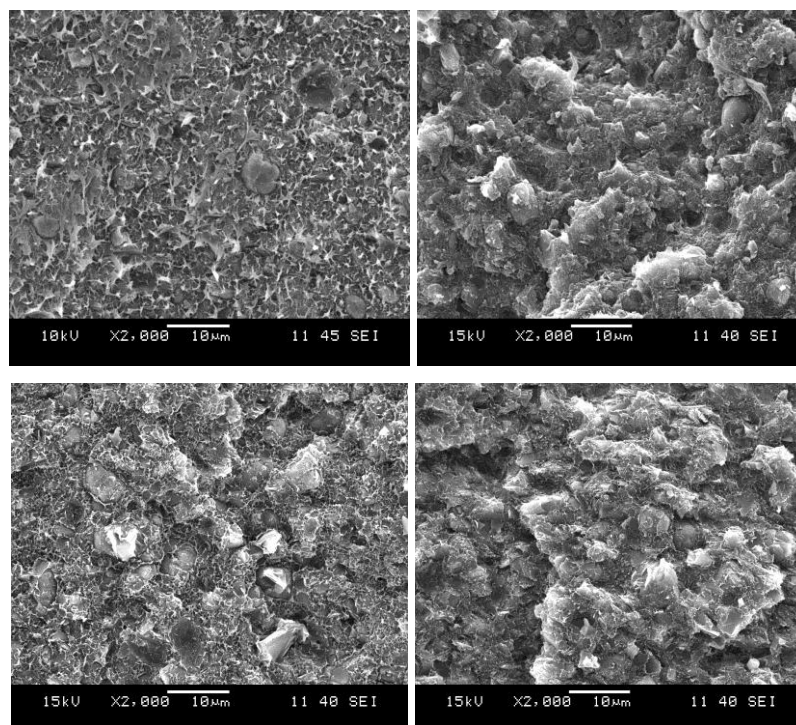


Figure 5.5 SEM images of HDPE/graphite, vol 2%, 5%, 10%, 16% graphite (magnification 2000x).

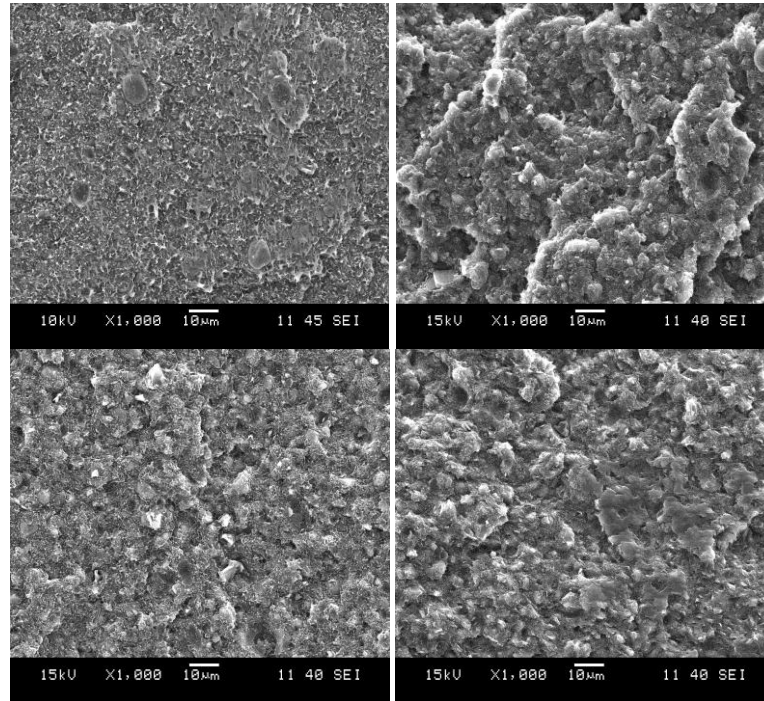


Figure 5.6 SEM images of HDPE/graphite, vol 2%, 5%, 10%, 16% graphite (magnification 1000x).

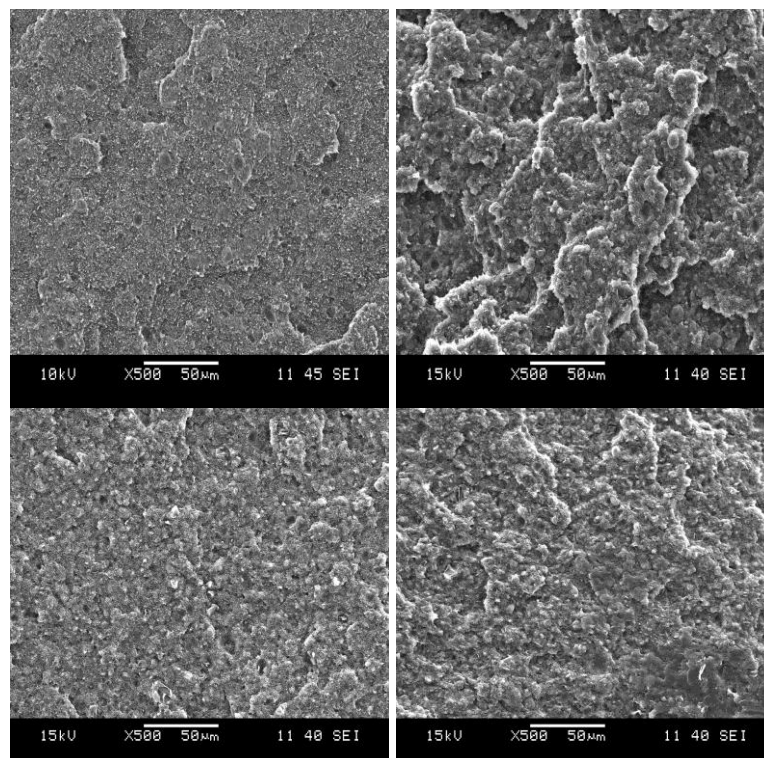


Figure 5.7 SEM images of HDPE/graphite, vol 2%, 5%, 10%, 16% graphite (magnification 500x).

CHAPTER SIX

CONCLUSIONS AND FUTURE REMARK

Graphite powder (400 nm) which has high thermal conductivity was mixed with HDPE in the Brabender Plasticorder mixer. Nanocomposites containing (2, 3, 4, 5, 6, 7, 10, 16 %) volume fractions of graphite were fabricated. To learn thermal conductivities, these samples were measured by hot disk method and with the increasing volume content of graphite it was observed that thermal conductivities were rose up nonlinearly, it was similar as in the literature. Besides, all theoretical models can not estimate the thermal conductivity of the composites in whole fractions. From the graph, it can be said until 6% volume fraction of graphite, results were closer to the theoretical models especially to Russell thermal conductivity model. Experimental results were compared with Maxwell, Russell, Lewis-Nielsen, Cheng-Vachon and geometric mean thermal conductivity models. By adding 2% volume content of graphite to HDPE, we obtain 0.55061 value of thermal conductivity (W/mK) and with the increasing percents of graphite we get 2.63906 value at the %16, intense increase was occurred. This rise is less apparent in the theoretical models.

Even the addition of small proportions of thermal conductive materials, they improve the thermal conductivity of composites.

Finally, samples' surface pictures were taken by scanning electron microscope in different magnifications (500x, 1000x, 2000x, 5000x). From the SEM examinations of polymer nanocomposites it can be expressed that graphite particles dispersed almost homogenously in polymer matrix.

In the future, studies must focus on making theoretical models that fit most new composites, have general validity for all composites.

REFERENCES

- Comparison of Thermal Properties.* (n.d). Retrieved May 12, 2011, from <http://www.skb.se/upload/publications/pdf/R-03-18webb.pdf>
- Graphite powder.* (n.d). Retrieved October 19, 2010, from <http://www.nanoamor.com/inc/sdetail/2345>
- Graphite's properties.* (n.d). Retrieved October 12, 2011, from <http://www.azom.com/article.aspx?ArticleID=1630>
- Hot-Disk.* (n.d). Retrieved May 12, 2011, from http://www.msm.cam.ac.uk/gordon/seminars/abstract_mich03.html
- Hot-Disk method.* (n.d). Retrieved July 13, 2010, from <http://www.hotdiskinstruments.com/home/technology.html>
- Instruction manual of Hot Disk software.* (n.d.). Instruction manual of Hot-Disk thermal constants analyser software version 5.9
- Krupa, I., Novák, I., & Chodák I. (2004). Electrically and thermally conductive polyethylene/graphite composites and their mechanical properties. *Synthetic Metals, 145*, 245–252. Retrieved October 25, 2010, from Science Direct database.
- Krupa, I., & Chodák, I. (2001). Physical properties of thermoplastic/graphite composites. *European Polymer Journal, 37*, 2159-2168. Retrieved October 25, 2010, from Science Direct database.
- Kumlucaş, D., Tavman, İ.H., & Çoban, M.T. (2003). Thermal conductivity of particle filled polyethylene composite materials. *Composites Science and Technology, 63*, 113-117. Retrieved September 29, 2010, from Science Direct database.

- Kumlutaş, D., & Tavman, İ.H. (2006). A numerical and experimental study on thermal conductivity of particle filled polymer composites. *Journal of Thermoplastic Composite Materials*, 19, 441-455. Retrieved November 8, 2010, from Sage database.
- Laser flash method.* (n.d). Retrieved May 12, 2010, from <http://www.evitherm.org/default.asp?lan=&ID=897&Menu1=897>
- Nanoage.* (n.d). Retrieved May 12, 2011, from <http://www.thenanoage.com/carbon.htm>
- Petkim-ürün özellikleri.* (n.d). Retrieved February 22, 2011, from <http://www.petkim.com.tr/Sayfa/1/41/URUNLER.aspx>
- Pradhan, N.R. (2010). *Thermal conductivity of nanowires, nanotubes and polymer nanotube composites.* Ph. D. Thesis. Worcester Polytechnic Institute, USA.
- Principal methods of thermal conductivity measurements.* (n.d.). Retrieved May 12, 2011, from <http://www.anter.com/TN67.htm>
- Polyethylene - high density (HDPE).* (n.d.). Retrieved May 25, 2011, from <http://www.icis.com/V2/chemicals/9076150/polyethylene-high-density.html>
- Sanada, K., Tada, Y., & Shindo, Y. (2009). Thermal conductivity of polymer composites with close-packed structure of nano and micro fillers. *Composites Part A, Applied Science and Manufacturing*, 40 (6-7), 724-730.
- Schadler, L.S., Brinson, L.C., & Sawyer, W.G. (2007). Polymer nanocomposites: A Small part of the story. *Journal of Metals*, 53-60.
- Tavman, İ.H. (1998). Effective thermal conductivity of isotropic polymer composites. *Int. Comm. Heat Mass Transfer*, 25 (5), 723-732.

- Tavman, İ.H., Çeçen, V., Özdemir, I., Turgut, A., Krupa, I., Omastova, M., & Novak, I. (2008). Preparation and characterization of highly electrically and thermally conductive polymeric nanocomposites. *Archives of Materials Science*, 29 (1-2), 77-83.
- Tekçe, H.S., Kumlutaş, D., & Tavman, İ.H. (2007). Effect of particle shape on thermal conductivity of copper reinforced polymer composites. *Journal of Reinforced Plastics and Composites*, 26 (1), 113-121.
- Thermal conductivity measurement methods*. (n.d.). Retrieved May 12, 2011, from <http://www.evitherm.org/default.asp?ID=308>
- Thermophysical properties*. (n.d.). Retrieved May 28, 2011, from [http://www.npl.co.uk/engineering-measurements/thermal/temperature/faqs/what-are-thermophysical-properties-\(faq-thermal\)](http://www.npl.co.uk/engineering-measurements/thermal/temperature/faqs/what-are-thermophysical-properties-(faq-thermal))
- Tlili, R., Boudenne, A., Cecen, V., Ibos, L., Krupa, I., & Candau, Y. (2010). Thermophysical and electrical properties of nanocomposites based on ethylene–vinylacetate copolymer (EVA) filled with expanded and unexpanded graphite. *Int J Thermophys*, 31, 936–948.
- Turgut, A. (2004). *A study on hot wire method of measuring thermal conductivity*. M.Sc. Thesis. Dokuz Eylül University, Turkey.
- Ye, C.M., Shentu, B.Q., & Weng, Z.X.(2006). Thermal conductivity of high density polyethylene filled with graphite. *Journal of Applied Polymer Science*, 101, 3806–3810.
- Zhang, X., Gu, H., & Fujii, M. (2006). Effective thermal conductivity and thermal diffusivity of nanofluids containing spherical and cylindrical nanoparticles. *Journal of Applied Physics*, 100, 044325.